⌘ *Author's Choice*

THE JOURNAL OF BIOLOGICAL CHEMISTRY VOL. 286, NO. 6, pp. 4809–4818, February 11, 2011

Endoplasmic Reticulum Stress Response Mediated by the PERK-eIF2α-ATF4 Pathway Is Involved in Osteoblast Differentiation Induced by BMP2*

Received for publication, June 8, 2010, and in revised form, October 26, 2010 Published, JBC Papers in Press, December 6, 2010, DOI 10.1074/jbc.M110.152900

Atsushi Saito[‡], Kimiko Ochiai[§], Shinichi Kondo[‡], Kenji Tsumagari[‡], Tomohiko Murakami[§], Douglas R. Cavener[¶], and Kazunori Imaizumi[‡1]

From the [‡]Department of Biochemistry, Division of Genome Radiobiology and Medical Science, Graduate School of Biomedical Science, University of Hiroshima, Hiroshima 734-8553, Japan, the [§]Division of Molecular and Cellular Biology, Department of Anatomy, Faculty of Medicine, University of Miyazaki, Miyazaki 889-1692, Japan, and the [¶]Department of Biology, Pennsylvania State University, University Park, Pennsylvania 16802

To avoid excess accumulation of unfolded proteins in the endoplasmic reticulum (ER), eukaryotic cells have signaling pathways from the ER to the cytosol or nucleus. These processes are collectively termed the ER stress response. Double stranded RNA activated protein kinase (PKR)-like endoplasmic reticulum kinase (PERK) is a major transducer of the ER stress response and directly phosphorylates eIF2α, resulting in translational attenuation. Phosphorylated eIF2α specifically promotes the translation of the transcription factor ATF4. ATF4 plays important roles in osteoblast differentiation and bone formation. *Perk*$^{-/-}$ mice are reported to exhibit severe osteopenia, and the phenotypes observed in bone tissues are very similar to those of *Atf4*$^{-/-}$ mice. However, the involvement of the PERK-eIF2α-ATF4 signaling pathway in osteogenesis is unclear. Phosphorylated eIF2α and ATF4 protein levels were attenuated in *Perk*$^{-/-}$ calvariae, and the gene expression levels of osteocalcin (*Ocn*) and bone sialoprotein (*Bsp*), which are targets for ATF4, were also down-regulated. Treatment of wild-type primary osteoblasts with BMP2, which is required for osteoblast differentiation, induced ER stress, leading to an increase in ATF4 protein expression levels. In contrast, the level of ATF4 in *Perk*$^{-/-}$ osteoblasts was severely diminished. The results indicate that PERK signaling is required for ATF4 activation during osteoblast differentiation. *Perk*$^{-/-}$ osteoblasts exhibited decreased alkaline phosphatase activities and delayed mineralized nodule formation relative to wild-type cultures. These abnormalities were almost completely restored by the introduction of ATF4 into *Perk*$^{-/-}$ osteoblasts. Taken together, ER stress occurs during osteoblast differentiation and activates the PERK-eIF2α-ATF4 signaling pathway followed by the promotion of gene expression essential for osteogenesis, such as *Ocn* and *Bsp*.

The endoplasmic reticulum (ER)[2] is a critical cellular compartment involved in the localization and folding of secreted and transmembrane proteins (1, 2). A number of cellular stress conditions lead to the accumulation of unfolded or misfolded proteins in the ER lumen, thereby representing a fundamental threat to cell viability. To avoid the excessive accumulation of unfolded proteins in the ER, eukaryotic cells have signaling pathways from the ER to the cytosol or nucleus. This process is referred to as the unfolded protein response (UPR) (3, 4). The UPR consists of the following three pathways: 1) suppression of protein translation to prevent the generation of more unfolded proteins; 2) facilitation of the refolding of unfolded proteins by the induction of ER molecular chaperones; and 3) activation of the ER-associated degradation to remove unfolded proteins that have accumulated in the ER by the ubiquitin-proteasome pathway. If these strategies fail, cells go into ER stress-induced apoptosis.

ER stress transducers have important roles in UPR signal transduction. The three major transducers of the UPR are PERK (PKR-like endoplasmic reticulum kinase) (5), IRE1 (inositol-requiring 1) (6, 7), and ATF6 (activating transcription factor 6) (8, 9). These three transducers sense the presence of the unfolded proteins in the ER lumen and transduce signals to the cytosol or nucleus. Activation of PERK leads to the phosphorylation of the α-subunit of the eukaryotic initiation factor 2 (eIF2α), which inhibits the assembly of the 80 S ribosome and inhibits protein synthesis (5, 10). In contrast to most proteins, ATF4 (activating transcription factor 4) escapes translational attenuation by eIF2α phosphorylation because ATF4 has upstream open reading frames (ORFs) in its 5′-untranslated region. These upstream ORFs, which prevent translation of the true ATF4 under normal conditions, are bypassed only when eIF2α is phosphorylated, and therefore ATF4 translation occurs (11, 12).

* This work was partly supported by grants from the Japan Society for the Promotion of Science KAKENHI (Grants 22020030, 21790323, 21790174, and 22800049), the Mochida Memorial Foundation for Medical and Pharmaceutical, the Senri Life Science Foundation, The Uehara Memorial Foundation, the Toray Science Foundation, and the Takeda Science Foundation.

⌘ *Author's Choice*—Final version full access.

[1] To whom correspondence should be addressed: 1-2-3 Kasumi, Minami-ku, Hiroshima 734-8553, Japan. Tel.: 81-82-257-5130; Fax: 81-82-257-5134; E-mail: imaizumi@hiroshima-u.ac.jp.

[2] The abbreviations used are: ER, endoplasmic reticulum; PERK, PKR-like endoplasmic reticulum kinase; ATF, activating transcription factor; OCN, osteocalcin; BSP, bone sialoprotein; UPR, unfolded protein response; IRE1, inositol-requiring 1; CREB, cAMP-responsive element-binding protein; TG, thapsigargin; BMP2, bone morphogenetic protein 2; ALP, alkaline phosphatase; OG2, osteocalcin gene 2; QRT-PCR, quantitative real-time PCR; P4, postnatal day 4; PKR, double stranded RNA activated protein kinase; Trap, tartrate-resistant acid phosphatase; OASIS, Old Astrocyte Specifically Induced Substance.

ATF4 is a member of the cAMP-responsive element-binding protein (CREB) family of basic zipper-containing proteins (13). A transcriptional target of ATF4 is osteocalcin (*Ocn*), which is osteoblast-specific and a marker for the late stage of osteoblast differentiation (14, 15). ATF4 is also required for preserving mature osteoblast function including the synthesis of collagen, the most abundant extracellular protein found in bones (16–18). Mice that are ATF4-deficient exhibit a marked reduction or delay in mineralization of bones including frontal and parietal bones, clavicles, and long bones (16). These observations clearly demonstrate that ATF4 is an essential transcription factor for osteoblast terminal differentiation and bone formation.

Loss of function mutations of *Perk* in humans and mice cause several neonatal developmental defects, including diabetes, growth retardation, and multiple skeletal dysplasia (19–23). Analyses on bone tissues revealed that $Perk^{-/-}$ mice show severe osteopenia, which is caused by a deficiency in the number of mature osteoblasts and impaired osteoblast differentiation. The phenotypes observed in bone tissues of $Perk^{-/-}$ mice are very similar to those of $Atf4^{-/-}$ mice. As mentioned, ATF4 is a translational target of activated PERK. Consequently, it is possible that bone phenotypes in $Perk^{-/-}$ mice are due to the loss of ATF4 activity, which is involved in osteoblast terminal differentiation and bone formation. Furthermore, a previous report showed that ER stress occurs during osteoblast differentiation (24), indicating that the PERK-eIF2α-ATF4 pathway may be involved in bone formation or osteoblast differentiation mediated by ER stress. In this study, we examined whether ATF4 expression and function are influenced by the loss of *Perk in vivo* and *in vitro* and confirm that ER stress during osteoblast differentiation activates PERK-eIF2α-ATF4 signaling followed by the promotion of gene expression essential for osteogenesis such as *Ocn* and bone sialoprotein (*Bsp*).

EXPERIMENTAL PROCEDURES

Mice and Cell Cultures—$Perk^{-/-}$ mice were generated as described previously (25). Primary cultured osteoblasts were prepared from the calvariae of postnatal day 4 (P4) wild-type (WT) and $Perk^{-/-}$ mice. The calvariae were digested with 0.1% collagenase (Wako) and 0.2% dispase (Invitrogen). Primary osteoblasts were grown in α modified Eagle's medium supplemented with 10% fetal calf serum at a density of 1.5×10^5 cells/well in 12-well plates. The medium was changed every 3 days and on the day of the assays to create identical conditions in each dish. We used thapsigargin (TG) (1 μM) (Wako) as an ER stressor for the indicated times and bone morphogenetic protein 2 (BMP2) (100 ng/ml) (Sigma) for osteoblast maturation (26).

RT-PCR—Total RNA was isolated from calvariae using an RNeasy mini kit (Qiagen) according to the manufacturer's protocol. First-strand cDNA was synthesized in a 20-μl reaction volume using a random primer (Takara) and Moloney murine leukemia virus reverse transcriptase (Invitrogen). PCR was performed in a total volume of 30 μl containing 0.8 μM of each primer, 0.2 mM dNTPs, 3 units of *Taq* polymerase, and 10× PCR buffer (Stratagene) using each specific primer set (Table 1). The PCR products were resolved by electrophoresis using a 4.8% acrylamide gel.

TABLE 1
Quantitative real-time PCR and RT-PCR were performed using each specific primer set
fwd, forward; rev, reverse.

Quantitative Real Time PCR
***Ocn*-fwd CTGACAAAGCCTTCATGTCCAA**
***Ocn*-rev GCGCCGGAGTCTGTTCACTA**
***Bsp-fwd* ACCGAGCTTATGAGGCGAA**
***Bsp-rev* GGGAATTCAAATGGGGAAAT**
***Opn*-fwd CACCCTGTTGCCCAGCTT**
***Opn*-rev TGCCCTTTCCGTTGTTGTC**
***Asns*-fwd CAAGGAGCCCAAGTTCAGTAT**
***Asns*-rev GGCTGTCCTCCAGCCAAT**
***Glyt1*-fwd TCATGGCTTTGTCGTCTGTCAT**
***Glyt1*-rev GCGGCAGAGCTGGAACA**
***Bip*-fwd AGCCATCCCGTGGCATAA**
***Bip*-rev GCACAGCGGCACCATAGG**
***Atf4*-fwd GCATGCTCTGTTTCGAATGGA**
***Atf4*-rev CCAACGTGGTCAAGAGCTCAT**
***Perk*-fwd TCTTGGTTGGGTCTGATGAAT**
***Perk*-rev GATGTTCTTGCTGTAGTGGGGG**
***β-actin*-fwd GACGGCCAGGTCATCATAT**
***β-actin*-rev AAGGAAGGCTGGAAAAGAGC**
RT-PCR
***Bip*-fwd GTTTGCTGAGGAAGACAAAAAGCTC**
***Bip*-rev CACTTCCATAGAGTTTGCTGATAAT**
***Xbp1*-fwd ACACGCTTGGGAATGGACAC**
***Xbp1*-rev CCATGGGAAGATGTTCTGGG**
***Trap-fwd* AAATCACTCTTTAAGACCAG**
***Trap-rev* TTATTGAATAGCAGTGACAG**
***Procollagen1a1*-fwd CCCCAACCCTGGAAACAGAC**
***Procollagen1a1*-rev GGTCACGTTCAGTTGGTCAAAGG**
***β-actin*-fwd TCCTCCCTGGAGAAGAGCTAC**
***β-actin*-rev TCCTGCTTGCTGATCCACAT**

Quantitative Real-time PCR—Total RNA was isolated from calvariae using an RNeasy mini kit (Qiagen) according to the manufacturer's protocol. First-strand cDNA was synthesized in a 20-μl reaction volume using a random primer (Takara) and Moloney murine leukemia virus reverse transcriptase (Invitrogen). Real-time quantitative RT-PCR reactions were run on an ABI Prism 7000 sequence detection system (Applied Biosystems) using the GoTaq quantitative PCR master

mix (Promega). Relative mRNA levels of all genes were first normalized to the levels of β-actin and then normalized to the average of WT levels. The primer sequences for the transcripts quantified by this method are shown (Table 1).

Western Blotting—For Western blotting, proteins were extracted from calvariae using a cell extraction buffer containing 10% SDS, 0.5 M EDTA at pH 8.0, 100 mM methionine, and a protease inhibitor mixture (MBL International). The lysates were incubated on ice for 45 min. After centrifugation at 16,000 × *g* for 15 min, the soluble proteins in the extracts were quantified. Samples were loaded onto sodium dodecyl sulfate-polyacrylamide gels. Protein-equivalent samples were subjected to Western blotting. The following antibodies were used: anti-β-actin (Sigma; 1:3000), anti-procollagen type I (Santa Cruz Biotechnology; 1:500), anti-OCN (Santa Cruz Biotechnology; 1:1000), anti-BSP (COSMO BIO; 1:1000), anti-ATF4 (Santa Cruz Biotechnology; 1:1000), anti-phospho-eIF2α (StressGen; 1:1000), anti-eIF2α (Cell Signaling; 1:1000), anti-phospho-PERK (Cell Signaling; 1:500), anti-PERK (Santa Cruz Biotechnology; 1:500), anti-phospho-GCN2 (Cell Signaling; 1:500), and anti-phospho-PKR (Millipore; 1:500).

Alizarin Red and Alkaline Phosphatase Staining—For the mineralization analysis, primary osteoblasts were stimulated by ascorbic acid (50 μg/ml), β-glycerophosphate (2 mM), and BMP2 (100 ng/ml) for 4 days. Alizarin red and alkaline phosphatase (ALP) staining were performed according to standard protocols. To quantify matrix mineralization, alizarin red-stained cultures were incubated with cetylpyridinium chloride (100 mM). The absorbance of the released alizarin red was measured at 570 nm. ALP activities were measured using the LabAssay ALP kit (Wako).

Morphological Analysis—For histological analysis, tibias were fixed in 10% formalin and then decalcified with 10% EDTA. Hematoxylin-eosin staining was performed using paraffin sections (6-μm) according to standard protocols. The thickness of cortical bones was measured in three sections of cortical bones. Tartrate-resistant acid phosphatase (Trap) staining was performed using a kit (Sigma). The number of Trap-positive cells was counted in three sections of a tibia.

Electron Microscopy—For histological analysis, tibiae were fixed in 2.5% glutaraldehyde, decalcified in a 10% EDTA-Na_2 solution, and post-fixed in 2% osmium tetroxide. The tibiae were visualized using a JEM-1200EX electron microscope (JEOL) operating at 80 kV.

Luciferase Assay—Reporter plasmids of p657 mOG2-Luc (where mOG2 is mouse osteocalcin gene 2), p6 OSE2-Luc, and p4 OSE1-Luc were kindly gifted from Guozhi Xiao (University of Pittsburgh). Osteoblasts were grown to 80% confluence in 24-well plates and then transfected with the Lipofectamine 2000 reagent according to the manufacturer's protocol (Invitrogen). Cells were transfected with a reporter plasmid (0.2 μg) carrying the firefly luciferase gene and the reference plasmid pRL-SV40 (0.02 μg) carrying the *Renilla* luciferase gene under the control of the SV40 enhancer and promoter (Promega). The cells were also transfected with a protein expression plasmid (0.2 μg) (pcDNA 3.1 (+); Invitrogen). After 30 h, the cells were lysed in 200 μl of Passive Lysis buffer (Promega). Cells were treated with TG (1 μM) for 12 h to induce ER stress and with BMP2 (100 ng/ml) for 48 h for osteoblast maturation before harvesting. The firefly and *Renilla* luciferase activities were measured in 10-μl cell lysates using a Dual-Luciferase reporter assay system (Promega) and a luminometer (Berthold Technologies). The relative luciferase activities were defined as the ratio of firefly luciferase activity to that of *Renilla* luciferase activity. The values were averaged from quadruplicate determinations in three independent experiments.

Statistic—Data are presented as the mean ± S.D. The statistical significance of differences was evaluated using the Student's *t* test.

RESULTS

Osteopenia in $Perk^{-/-}$ Mice—Bone formation was impaired in the long and flat bones of $Perk^{-/-}$ mice skeletons, indicating that both intramembranous and endochondral ossification were defective. In particular, cortical bones in long bones were much thinner than those of WT mice (Fig. 1, *A* and *B*). The expression of PERK has been reported to be high in bone tissues (25). We examined what types of cells express PERK using primary cultures of osteoblasts and osteoclasts. High levels of *Perk* mRNA were expressed in primary osteoblasts; however, in osteoclasts, this was not the case (Fig. 1, *G* and *H*). Electron microscopic analysis using ultrathin sections of long bones (femur) revealed that the osteoblasts of $Perk^{-/-}$ mice have abnormally enlarged rough ER with materials retained in the lumen (Fig. 1*C*). In addition, primary cultured osteoblasts prepared from $Perk^{-/-}$ calvariae exhibited an even more pronounced elevation of procollagen type I levels in the cytosol when compared with WT littermates (Fig. 1*D*). This finding suggests that the materials observed in the abnormally enlarged rough ER of $Perk^{-/-}$ mice correspond to unprocessed procollagen, and there is a reduction in the mature type I collagen secretion from the ER to extracellular regions. The number of Trap-positive cells of osteoclasts was not significantly different when compared with the WT mice (Fig. 1, *E* and *F*). These results suggest that osteopenia in the osseous tissues of $Perk^{-/-}$ mice may primarily be caused by osteoblast dysfunction.

Downstream Gene and Protein Expression of PERK in Bone Tissues of $Perk^{-/-}$ Mice—To examine whether the expression of ATF4 is influenced by the loss of *Perk*, we examined the expression of *Atf4* mRNA and ATF4 protein levels in bone tissues. Although the *Atf4* mRNA levels in $Perk^{-/-}$ bones were comparable with those of the WT mice (Fig. 1*I*), translated ATF4 levels were markedly reduced, with levels of only 35% when compared with WT mice (Fig. 1*J*). *Ocn* and *Bsp*, which are targets of ATF4, were also significantly reduced at the transcriptional and translational levels (Fig. 1, *I* and *J*), indicating that ATF4 and its downstream targets are impaired in $Perk^{-/-}$ mice. Up-regulated ATF4 protein in response to ER stress is known to promote the expression of genes that are associated with amino acid import and metabolism, such as asparagine synthase (*Asns*) and glycine transporter 1 (*Glyt1*) (27). The levels of these genes were also slightly reduced in $Perk^{-/-}$ bone tissues when compared with the levels observed in WT mice (Fig. 1*I*). Levels of phosphory-

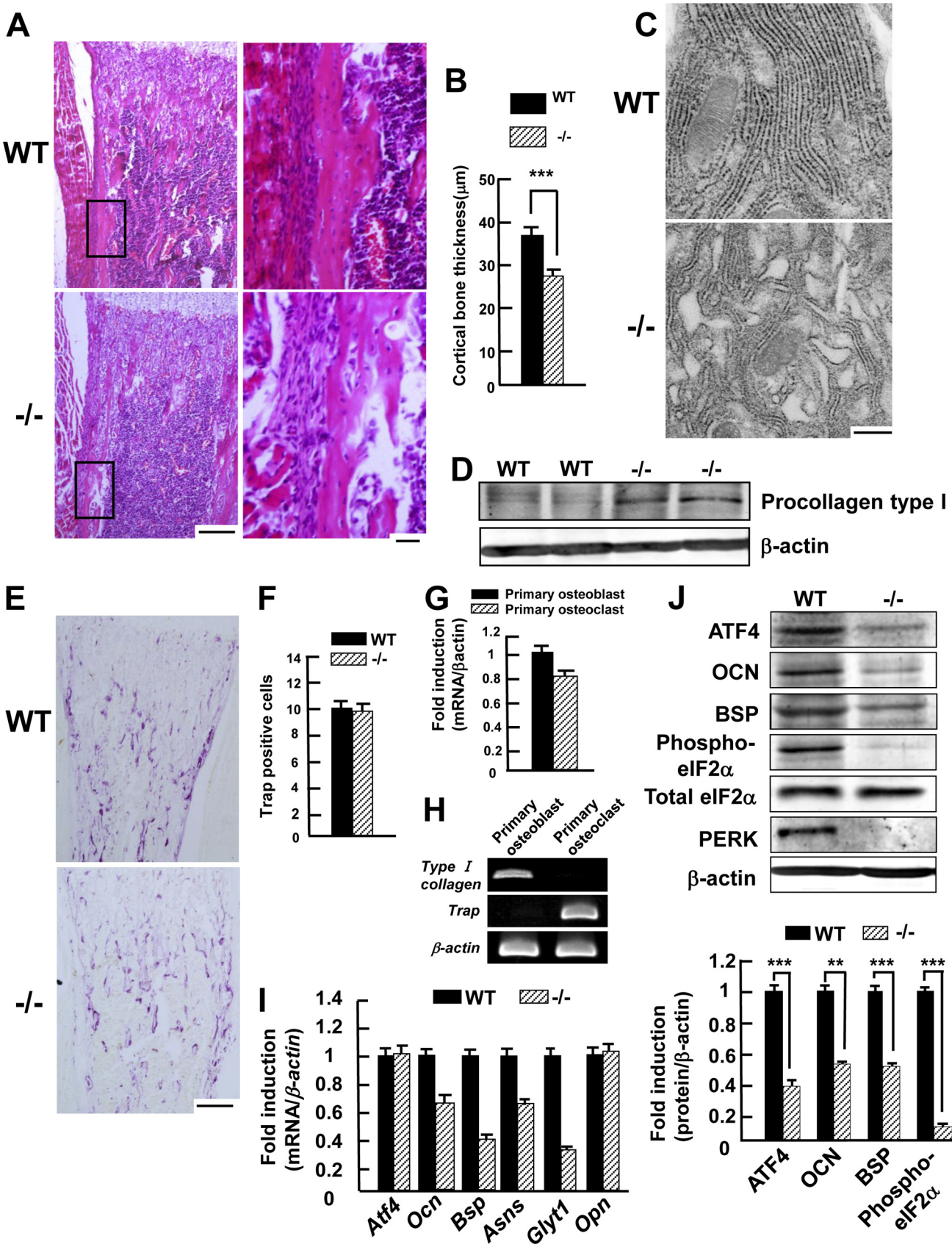
A
WT
-/-
B
WT
-/-
***
Cortical bone thickness(μm)
50
40
30
20
10
0
C
WT
-/-
D
WT WT -/- -/-
Procollagen type I
β-actin
E
WT
-/-
F
WT
-/-
Trap positive cells
14
12
10
8
6
4
2
0
G
Primary osteoblast
Primary osteoclast
Fold induction (mRNA/βactin)
1.2
1
0.8
0.6
0.4
0.2
0
H
Primary osteoblast
Primary osteoclast
Type I collagen
Trap
β-actin
I
WT
-/-
Fold induction (mRNA/β-actin)
1.4
1.2
1
0.8
0.6
0.4
0.2
0
Atf4
Ocn
Bsp
Asns
Glyt1
Opn
J
WT -/-
ATF4
OCN
BSP
Phospho-eIF2α
Total eIF2α
PERK
β-actin
WT
-/-
Fold induction (protein/β-actin)
1.2
1
0.8
0.6
0.4
0.2
0
***
**
***
***
ATF4
OCN
BSP
Phospho-eIF2α

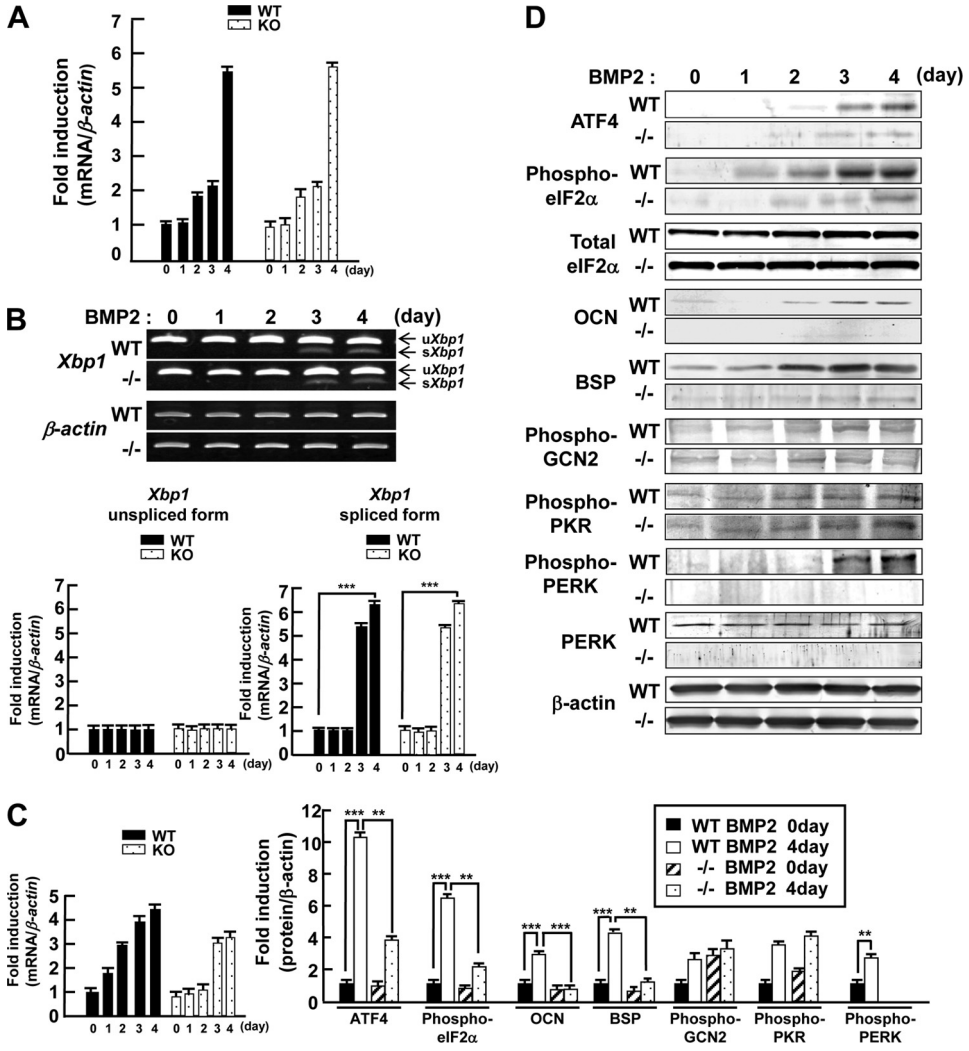

FIGURE 2. **The PERK-eIF2α-ATF4 signaling pathway was impaired in *Perk*$^{-/-}$ osteoblasts treated with BMP2.** *A*, QRT-PCR analysis of *Bip* mRNA in primary osteoblasts prepared from P4 WT and *Perk*$^{-/-}$ calvariae. The osteoblasts were treated with BMP2 (100 ng/ml) for the indicated times. The expression levels of *Bip* mRNA were almost equal in WT and *Perk*$^{-/-}$ osteoblasts. *B*, RT-PCR analysis of *Xbp1* in primary osteoblasts prepared from P4 WT and *Perk*$^{-/-}$ calvariae. The osteoblasts were treated with BMP2 (100 ng/ml) for the indicated times. The expression levels of unspliced forms of *Xbp1* mRNA (*uXbp1*) and spliced forms of *Xbp1* mRNA (*sXbp1*) mRNA were essentially equal in WT and *Perk*$^{-/-}$ osteoblasts. *Lower panels* show the quantitative analysis of the mRNA expression levels (mean ± S.D. $n = 3$, ***, $p < 0.001$; Student's *t* test). *C*, QRT-PCR analysis of *Asns* mRNA in primary osteoblasts prepared from P4 WT and *Perk*$^{-/-}$ calvariae treated with BMP2 for the indicated times. The expression levels of *Asns* were suppressed in *Perk*$^{-/-}$ osteoblasts. *D*, Western blotting analysis of primary osteoblasts prepared from P4 WT and *Perk*$^{-/-}$ calvariae. The osteoblasts were treated with BMP2 (100 ng/ml) for the indicated times. The expression levels of ATF4, phosphorylated eIF2α, OCN, and BSP proteins were gradually up-regulated after treatment with BMP2 in WT primary osteoblasts. In contrast, the induction of these proteins was severely inhibited in *Perk*$^{-/-}$ primary osteoblasts. The *lower panel* shows the quantitative analysis of the protein expression levels (mean ± S.D., $n = 3$, **, $p < 0.01$, ***, $p < 0.001$; Student's *t* test).

lated eIF2α should be equally reduced if the decrease in the levels of expression of ATF4 target genes is due to a defect of PERK-ATF4 signaling. Although the total amount of eIF2α did not change, the level of phosphorylated eIF2α was significantly reduced (Fig. 1*J*). Taken together, these results suggest that the expression of eIF2α, ATF4, and the downstream targets of ATF4 are influenced by the PERK deficiency in bone tissues.

FIGURE 1. **Morphological changes in bone tissues and gene expression in *Perk*$^{-/-}$ mice.** *A*, hematoxylin-eosin staining of femurs in P4 wild-type (WT) and *Perk*$^{-/-}$ (−/−) mice. *Right panels* are a higher magnification of the *boxed areas* in the *left panels*. *Scale bars*, 100 μm (*left*), 20 μm (*right*). *B*, the panel shows the quantification of the thickness of cortical bones. Note that the cortical bone of *Perk*$^{-/-}$ mice is extremely thin (mean ± S.D., $n = 3$, ***, $p < 0.001$; Student's *t* test). *C*, electron microscopy images of osteoblasts in femur cortical bones of P4 WT (*upper*) and *Perk*$^{-/-}$ (*lower*) mice. In *Perk*$^{-/-}$ osteoblasts, the rough ER was abnormally expanded. *Scale bar*, 1 μm. *D*, Western blotting analysis of procollagen Type I in primary osteoblasts prepared from WT and *Perk*$^{-/-}$ calvariae. *E*, Trap staining of femurs in P4 WT (*top*) and *Perk*$^{-/-}$ (*bottom*) mice. *Scale bar*, 100 μm. *F*, the number of osteoclasts did not significantly change in *Perk*$^{-/-}$ mice when compared with WT mice. *G*, quantitative real-time PCR (QRT-PCR) analysis of *Perk* in primary osteoblasts and osteoclasts prepared from P4 WT mice calvariae. Primary osteoblasts showed high levels of *Perk* mRNA expression, whereas osteoclasts did not show high expression levels. *H*, RT-PCR analysis of type I collagen (a marker of osteoblast) and *Trap* (a marker of osteoclast) in primary osteoblasts and osteoclasts prepared from P4 WT mice calvariae. *I*, QRT-PCR analysis using mRNA extracted from P4 WT and *Perk*$^{-/-}$ calvariae. The expression levels of *Ocn*, *Bsp*, *Asns*, and *Glyt1* mRNAs were suppressed in *Perk*$^{-/-}$ calvariae. *J*, Western blotting using proteins extracted from P4 WT and *Perk*$^{-/-}$ calvariae. The expression levels of ATF4, OCN, BSP, and phosphorylated eIF2α proteins were suppressed in *Perk*$^{-/-}$ calvariae. The *lower panel* shows the quantitative analysis of the protein expression levels (mean ± S.D., $n = 3$, **, $p < 0.01$; ***, $p < 0.001$; Student's *t* test).

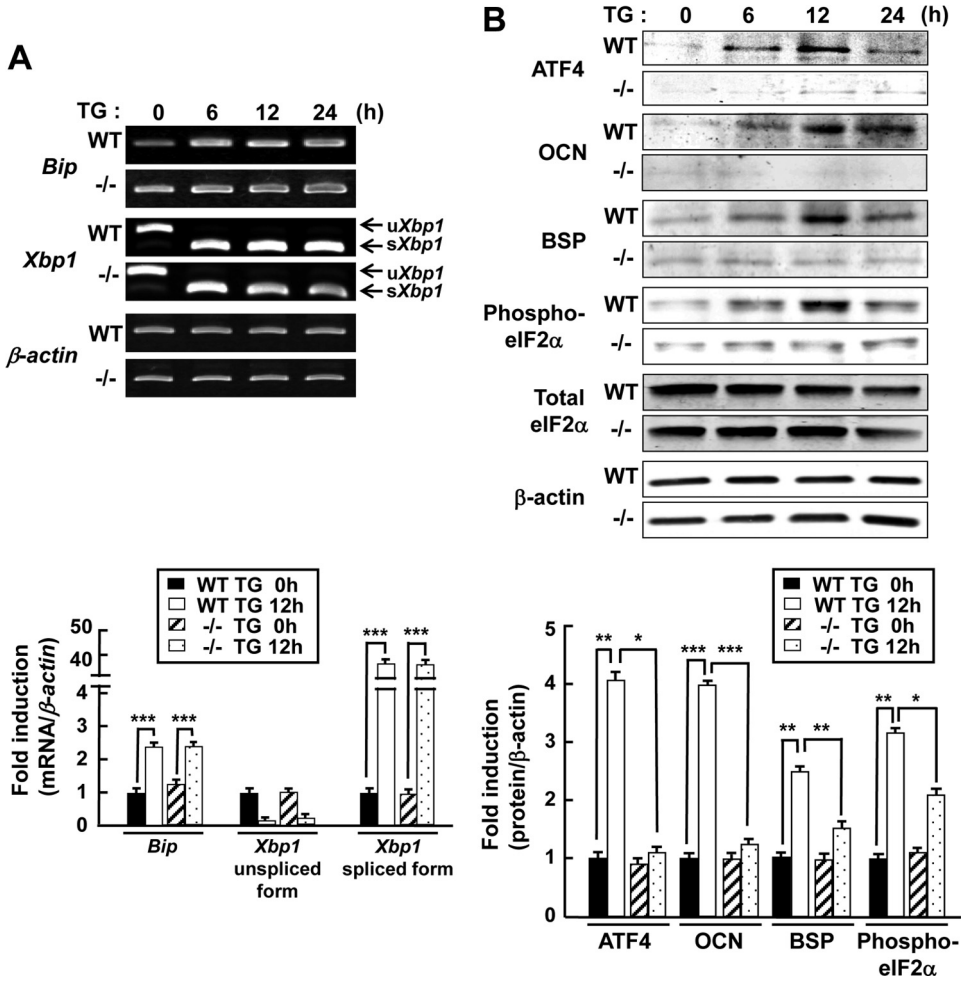

FIGURE 3. **Impaired activation of the PERK-eIF2α-ATF4 pathway by ER stress in *Perk*$^{-/-}$ osteoblasts.** *A*, RT-PCR analysis of UPR-related genes in primary osteoblasts prepared from P4 WT and *Perk*$^{-/-}$ calvariae. The osteoblasts were exposed to thapsigargin (TG; 1 μM), which is an ER stressor, for the indicated times. The expression levels of *Bip* and spliced forms of *Xbp*1 mRNA (*sXbp1*) were almost equal in WT and *Perk*$^{-/-}$ osteoblasts. The *lower panel* shows the quantitative analysis of the mRNA expression levels (mean ± S.D., $n = 3$, ***, $p < 0.001$; Student's *t* test). *uXbp1*, unspliced forms of *Xbp1* mRNA. *B*, Western blotting analysis of primary osteoblasts prepared from P4 WT and *Perk*$^{-/-}$ calvariae. The osteoblasts were exposed to TG (1 μM) for the indicated times. The expression levels of ATF4, OCN, BSP, and phosphorylated eIF2α proteins were suppressed in *Perk*$^{-/-}$ osteoblasts when compared with WT osteoblasts. The *lower panel* shows the quantitative analysis of the protein expression levels (mean ± S.D., $n = 3$, *, $p < 0.05$, **, $p < 0.01$, ***, $p < 0.001$; Student's *t* test).

The PERK-eIF2α-ATF4 Pathway Is Activated by BMP2—We previously reported that treatment of immature osteoblasts with BMP2, which is required for osteoblast differentiation and bone formation, induces mild ER stress (24). To confirm this, the expression of ER stress markers when primary calvarial osteoblasts were treated with BMP2 was examined. *Bip* mRNA was gradually up-regulated, and spliced forms of X-box-binding protein 1 (*Xbp1*) mRNA were also detected in both WT and *Perk*$^{-/-}$ osteoblasts (Fig. 2, *A* and *B*), indicating that ER stress actually occurs after treatment with BMP2, and normal UPR signaling is activated in response to ER stress induced by BMP2 in both WT and *Perk*$^{-/-}$ cells. In contrast, the level of *Asns* was slightly reduced in *Perk*$^{-/-}$ osteoblasts under these conditions (Fig. 2*C*). We then investigated whether the PERK-eIF2α-ATF4 pathway is activated by BMP2. In the WT osteoblasts, treatment with BMP2 caused phosphorylation of eIF2α, and ATF4 protein levels were also elevated (Fig. 2*D*). In contrast, eIF2α and ATF4 were not activated in *Perk*$^{-/-}$ osteoblasts (Fig. 2*D*). OCN and BSP, which are downstream of ATF4, were up-regulated in WT cells but not in *Perk*$^{-/-}$ cells (Fig. 2*D*). Other protein kinases such as PKR and GCN2 are known to couple distinct upstream stress signals to eIF2α phosphorylation (28, 29). Activation of the eIF2α-ATF4 pathway in *Perk*$^{-/-}$ osteoblasts after treatment with BMP2 may be due to other kinases. Consequently, phosphorylated levels of PKR and GCN2 were measured. Phosphorylated PKR and GCN2 were at comparable levels in both WT and *Perk*$^{-/-}$ osteoblasts (Fig. 2*D*). These data indicate that treatment of calvarial osteoblasts with BMP2 induces ER stress followed by the activation of the PERK-eIF2α-ATF4 pathway, and the signaling promotes the expression of ATF4 targets, OCN and BSP, which are mature osteoblast markers. In contrast, this signaling pathway is impaired in *Perk*$^{-/-}$ osteoblasts.

Alternatively, we analyzed whether the expression of OCN and BSP is increased in an ER stress-dependent manner. Treatment with the ER stressor TG, an inhibitor of ER Ca^{2+}-ATPase, rapidly induced *Bip* mRNA and spliced forms of *Xbp1* mRNA (Fig. 3*A*). At the same time, ATF4 translation was promoted, and protein levels of its downstream targets,

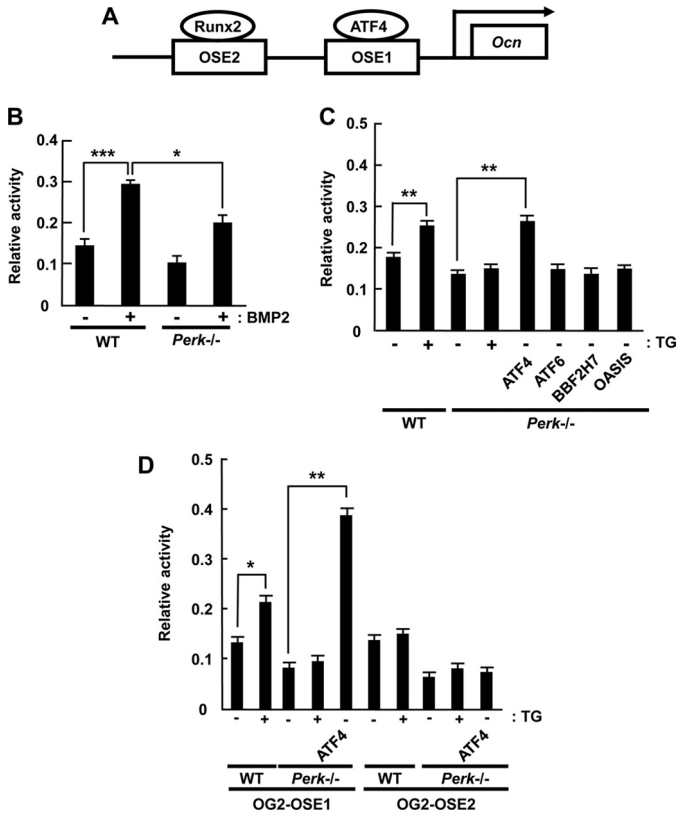

FIGURE 4. **The activation of the OSE1 promoter region mediated by ATF4 is inhibited in *Perk*$^{-/-}$ osteoblasts.** *A*, scheme of the promoter region of mouse OG2 (*Ocn* promoter) that includes the OSE2 (Runx2 binding site) and OSE1 (ATF4 binding site) regions. *B*, reporter assays using the OG2 promoter. Primary osteoblasts were transfected with the OG2 reporter construct and treated with or without BMP2 (100 ng/ml). In *Perk*$^{-/-}$ osteoblasts treated with BMP2, the reporter activities were reduced when compared with WT osteoblasts. Data are presented as the ratio of firefly luciferase activities to *Renilla* luciferase activities (mean ± S.D., $n = 3$, *, $p < 0.05$, ***, $p < 0.001$; Student's *t* test). *C*, reporter assays using OG2 promoter and indicated constructs. The reporter activities were observed to increase upon exposure to TG (1 μM) in WT primary osteoblasts but not in *Perk*$^{-/-}$ osteoblasts. Note that the reporter activities increased significantly when ATF4 was introduced to *Perk*$^{-/-}$ osteoblasts. The introduction of other CREB/ATF family members did not induce the reporter activities (mean ± S.D., $n = 3$, **, $p < 0.01$; Student's *t* test). *D*, reporter assays using OG2-OSE1 and OG2-OSE2. The reporter activities of WT primary osteoblasts transfected with the OG2-OSE1 reporter were induced by exposure to TG (1 μM) but not with OSE2 (mean ± S.D., $n = 3$, *, $p < 0.05$, **, $p < 0.01$; Student's *t* test). OASIS (Old Astrocyte Specifically Induced Substance).

OCN and BSP, were significantly increased in WT osteoblasts but not in *Perk*$^{-/-}$ cells (Fig. 3*B*). Taken together, ER stress may be sufficient for the up-regulation of mature osteoblast markers mediated by ATF4 translation, but loss of *Perk* eliminates induction of ATF4 target osteoblast markers by ER stress or BMP2.

Loss of Perk Causes a Decrease in the Promoter Activities of OSE1 Mediated by ATF4—Two osteoblast-specific cis-acting elements are present in the *Ocn* promoter (14, 15). One of these elements is OSE2, which is the binding site for Runx2 (30, 31). OSE1 is the second cis-acting element and the binding site for ATF4 (Fig. 4*A*) (14, 15). To confirm that the decrease in *Ocn* mRNA in *Perk*$^{-/-}$ osteoblasts is due to ATF4 dysfunction, we performed reporter assays using a reporter gene (OG2) carrying a 670-bp promoter of *Ocn* that includes both OSE1 and OSE2. The reporter activities of OG2 were significantly up-regulated by the treatment of WT calvarial osteoblasts with BMP2, whereas in *Perk*$^{-/-}$ cells, the activities were significantly reduced (Fig. 4*B*). The OG2 reporter activities were examined when cells were exposed to the ER stressor, TG. The reporter activities were significantly increased following the treatment of WT cells with TG, whereas the activities showed no increase in *Perk*$^{-/-}$ cells (Fig. 4*C*). When cells were transfected with the ATF4 expression vector, the reporter activities in *Perk*$^{-/-}$ cells increased to the levels in WT cells that were treated with TG. However, the other CREB/ATF family members, ATF6, Old Astrocyte Specifically Induced Substance (OASIS), and BBF2H7 (32), could not restore the reporter activities (Fig. 4*C*).

To demonstrate that PERK signaling directly acts on the OSE1 of OG2, we used reporter genes carrying either the OG2 deleted OSE2 sequence (OG2-OSE1) or the OG2 deleted OSE1 sequence (OG2-OSE2). Treatment of WT calvarial osteoblasts with TG promoted the reporter activities of OG2-OSE1 but not the activities of OG2-OSE2 in WT osteoblasts (Fig. 4*D*). The OG2-OSE1 reporter activities were not promoted by the treatment of *Perk*$^{-/-}$ osteoblasts with TG. The activities were restored by the introduction of ATF4 in *Perk*$^{-/-}$ cells. In contrast, ATF4 expression could not promote the reporter activities of OG2-OSE2 in *Perk*$^{-/-}$ cells (Fig. 4*D*). These results indicate that the reduction of the *Ocn* promoter activities in *Perk*$^{-/-}$ osteoblasts is due to the impaired activation of the OSE1 site mediated by ATF4.

ATF4 Restores the Osteoblastic Function in Perk$^{-/-}$ *Osteoblasts—Perk*$^{-/-}$ osteoblast cultures showed delayed mineralized nodule formation and a decrease in alkaline phosphatase activity after treatment with BMP2, as reported previously (23) (Fig. 5, *B* and *C*). We examined whether these abnormalities were recovered by the introduction of ATF4. The protein levels of OCN and BSP were up-regulated following treatment with BMP2 in WT osteoblasts but did not increase in *Perk*$^{-/-}$ osteoblasts (Fig. 5*A*). Infection of *Perk*$^{-/-}$ cells with an adenovirus expressing ATF4 recovered the expression levels of OCN and BSP (Fig. 5*A*). Mineralized nodule formation and alkaline phosphatase activity after treatment with BMP2 were delayed in *Perk*$^{-/-}$ osteoblasts when compared with WT osteoblasts (Fig. 5, *B* and *C*). The delayed mineralized nodule formation and reduction in alkaline phosphatase activities were almost completely restored by the introduction of ATF4 into *Perk*$^{-/-}$ osteoblasts (Fig. 5, *B* and *C*). These results indicate that osteoblastic dysfunction in *Perk*$^{-/-}$ osteoblasts is because of the impaired activation of ATF4 and its downstream signaling targets.

DISCUSSION

Perk$^{-/-}$ mice showed severe osteopenia involving decreases in cortical and trabecular bone thickness, and these findings are similar to a previous report (23). Wei *et al.* (23) speculated that osteopenia in *Perk*$^{-/-}$ mice is caused by a deficiency in the number of mature osteoblasts, impaired osteoblast differentiation, and reduced type I collagen secretion. In this report, a decrease in the expression levels of mature osteoblast markers OCN and BSP was observed in *Perk*$^{-/-}$ osteoblast. In addition, collagen secretion and alkaline phospha-

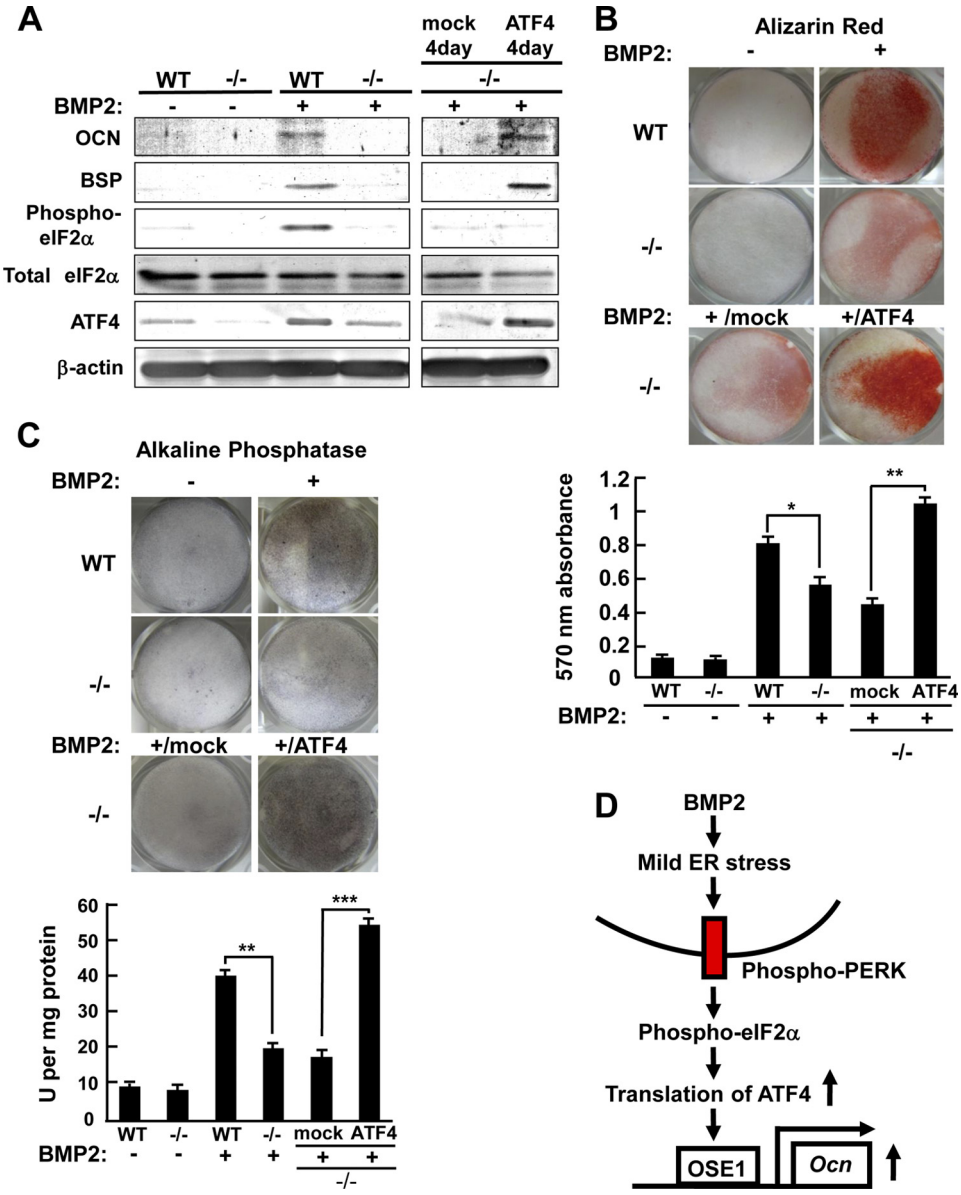

FIGURE 5. **The PERK-eIF2α-ATF4 pathway is involved in osteoblast differentiation.** *A*, Western blotting of primary osteoblasts infected with adenovirus expressing ATF4. The expression levels of OCN and BSP were restored by the introduction of ATF4 to *Perk*$^{-/-}$ osteoblasts. *mock* is an empty vector. *B*, mineralization nodule formation in WT and *Perk*$^{-/-}$ osteoblasts. WT and *Perk*$^{-/-}$ primary osteoblasts were treated with BMP2 for 0 or 4 days, and cells were stained with alizarin red for visualizing mineralization. The delayed mineralized nodule formation in *Perk*$^{-/-}$ osteoblasts was restored by the infection with an adenovirus expressing ATF4. The *lower panel* shows the quantitative analysis of alizarin red staining (mean ± S.D., $n = 4$, *, $p < 0.05$, **, $p < 0.01$; Student's *t* test). *C*, alkaline phosphatase activity in WT and *Perk*$^{-/-}$ primary osteoblasts. Cells were stained with 5-bromo-4-chloro-3-indolyl phosphate for measuring ALP activities. Although ALP activities were reduced in *Perk*$^{-/-}$ osteoblasts, they were restored by the introduction of ATF4 into *Perk*$^{-/-}$ osteoblasts. The *lower panel* shows the quantitative analysis of ALP activities (mean ± S.D., $n = 4$, **, $p < 0.01$, ***, $p < 0.001$; Student's *t* test). *D*, proposed model for the induction of ATF4 target osteoblast markers mediated by the PERK-eIF2α-ATF4 pathway during osteoblast differentiation.

tase activities were reduced in *Perk*$^{-/-}$ osteoblasts. Taken together, late phase maturation of osteoblasts is impaired in *Perk*$^{-/-}$ mice. *Atf4*$^{-/-}$ mice also exhibit severe osteopenia involving impaired osteoblast differentiation (16), and these findings are very similar to those observed for *Perk*$^{-/-}$ mice. ATF4 is a downstream molecule and a translational target of PERK. This signaling pathway plays an important role in the recovery of damaged cells exposed to ER stress. The observed similarity in the bone tissue or osteoblast phenotypes in both mice suggests that the PERK-ATF4 signaling pathway is associated with bone formation or osteoblast differentiation. In this study, the impact of the PERK-eIF2α-ATF4 signaling pathway on osteoblast biology was examined. We obtained significant data that indicated that this signaling pathway is involved in osteoblast biology as follows. 1) ATF4 protein levels were reduced in *Perk*$^{-/-}$ calvariae. 2) Targets of ATF4, OCN, and BSP, were down-regulated after treatment with BMP2 in *Perk*$^{-/-}$ primary calvarial cultures. 3) OSE1-dependent *Ocn* reporter activities in *Perk*$^{-/-}$ osteoblasts were lower when compared with WT osteoblasts. This reduction in reporter activities was restored by the introduction of ATF4. 4) Reduction of ALP activities and mineralization in *Perk*$^{-/-}$ osteoblasts were restored by the introduction of ATF4. These findings support the notion that the PERK-eIF2α-ATF4 sig-

naling pathway plays a role in BMP2-induced osteoblast differentiation and osteogenesis in culture (Fig. 5*D*).

In a previous report, ATF4 was found to be normally expressed along with its downstream amino acid metabolism genes in *Perk*$^{-/-}$ bone tissues (23). The report concluded that osteoblast defects in *Perk*$^{-/-}$ mice were not due to abnormal expression or activity of ATF4. This conclusion contrasts the results presented in this study. The reasons for this discrepancy are unclear; however, there are several important experimental differences between the previous reports and this report. One important point is that in the previous study, the mRNA was extracted from long bones for measuring the expression levels of ATF4 downstream genes. Although bone tissues were devoid of soft tissue and bone marrow, as set out under "Materials and Methods" in the previous study, it is possible that some types of cells other than those derived from bone tissues may have been present in the samples used (23). Thus, if such samples were used in experiments, it is possible that the results are affected. We have examined the expression of ATF4 and downstream genes in detail as follows. 1) We checked the expression of ATF4 and downstream genes that ATF4 regulates using calvarial bone tissues that did not include any other tissues or cells except bone cells such as osteoblasts, osteocytes, and osteoclasts. 2) We also checked the expression of these genes using primary cultured osteoblasts treated with BMP2. 3) The expression levels of these genes were subjected to quantitative analysis. The data showed that ATF4 protein levels were significantly reduced both in *Perk*$^{-/-}$ bone tissues and in primary osteoblasts and that downstream gene expression was also affected. It is unknown whether the expression levels of ATF4 downstream genes were negligibly down-regulated even if the levels of ATF4 expression significantly decreased in *Perk*$^{-/-}$ bones. *Asns* is an ATF4 downstream target under ER stress conditions. The expression levels of this gene are also affected under conditions without ER stress by other transcription factors such as CAAT/enhancer-binding protein β (C/EBPβ) (33). Therefore, even if the expression of ATF4 is low in *Perk*$^{-/-}$ cells, a second pathway may maintain the expression levels of such genes in bone tissues or osteoblasts under conditions where ER stress is absent.

To activate the PERK-eIF2α-ATF4 pathway, ER stress in osteoblasts is required. As shown in the present study, treatment of cranial immature osteoblasts with BMP2 induces mild ER stress involving the facilitation of osteogenesis. When immature osteoblasts are differentiating into mature forms, osteoblasts produce abundant proteins, and some of these proteins would transiently accumulate in the ER. Thus, it is possible that ER stress in osteoblasts treated with BMP2 is associated with a high demand for synthesis and secretion of bone matrix proteins. However, it is unknown whether ER stress actually occurs in differentiating osteoblasts and during osteogenesis *in vivo*. Additionally, the role of PERK-eIF2α-ATF4 signaling in osteobiology and osteogenesis *in vivo* is not clearly defined. Further examination is required to clarify the significance of ER stress signaling, including the PERK pathway, on bone formation.

Perk$^{-/-}$ osteoblasts have abnormally enlarged rough ER with materials contained within the lumen. Wei *et al.* (23) demonstrated that type I collagen is accumulated in the ER. From these findings, they speculated that type I collagen is not secreted to the extracellular space, leading to the suppression of bone matrix formation. The same findings were observed in the present study. Therefore, loss of PERK function leads to impaired protein folding in the ER or transport of the secreted materials from the ER to the Golgi body. This dysfunction disturbs the secretion of the bone matrix. There are no reports showing that *Atf4*$^{-/-}$ osteoblasts display morphological changes to the ER. Thus, it is possible that the abnormal expansion of the rough ER in the *Perk*$^{-/-}$ osteoblasts is independent of the impaired ATF4 pathway and may be caused by the down-regulation of other downstream molecules of PERK.

In conclusion, ER stress is induced during osteoblast differentiation and activates the PERK-eIF2α-ATF4 pathway. Translationally up-regulated ATF4 downstream of PERK facilitates OSE1-site dependent gene expression followed by the promotion of osteogenesis. Specific activation of the PERK-eIF2α-ATF4 pathway may represent therapeutic strategies against bone diseases such as osteogenesis imperfecta. To develop these strategies, a detailed understanding of the ATF4 targets and the importance of bone formation by this signaling pathway *in vivo* is necessary.

Acknowledgments—We thank Guozhi Xiao (University of Pittsburg, PA) for providing OG2 reporter plasmids and Ikuyo Tsuchimochi, Tomoko Kawanami, and Yukiko Motoura for technical support.

REFERENCES

1. Gething, M. J., and Sambrook, J. (1992) *Nature* **355,** 33–45
2. Ellgaard, L., Molinari, M., and Helenius, A. (1999) *Science* **286,** 1882–1888
3. Ron, D. (2002) *J. Clin. Invest.* **110,** 1383–1388
4. Rutkowski, D. T., and Kaufman, R. J. (2004) *Trends Cell Biol.* **14,** 20–28
5. Harding, H. P., Zhang, Y., and Ron, D. (1999) *Nature* **397,** 271–274
6. Tirasophon, W., Welihinda, A. A., and Kaufman, R. J. (1998) *Genes Dev.* **12,** 1812–1824
7. Calfon, M., Zeng, H., Urano, F., Till, J. H., Hubbard, S. R., Harding, H. P., Clark, S. G., and Ron, D. (2002) *Nature* **415,** 92–96
8. Yoshida, H., Okada, T., Haze, K., Yanagi, H., Yura, T., Negishi, M., and Mori, K. (2000) *Mol. Cell. Biol.* **20,** 6755–6767
9. Shen, J., Chen, X., Hendershot, L., and Prywes, R. (2002) *Dev. Cell* **3,** 99–111
10. Shi, Y., Vattem, K. M., Sood, R., An, J., Liang, J., Stramm, L., and Wek, R. C. (1998) *Mol. Cell. Biol.* **18,** 7499–7509
11. Harding, H. P., Novoa, I., Zhang, Y., Zeng, H., Wek, R., Schapira, M., and Ron, D. (2000) *Mol. Cell* **6,** 1099–1108
12. Vattem, K. M., and Wek, R. C. (2004) *Proc. Natl. Acad. Sci. U. S. A.* **101,** 11269–11274
13. Karpinski, B. A., Morle, G. D., Huggenvik, J., Uhler, M. D., and Leiden, J. M. (1992) *Proc. Natl. Acad. Sci. U. S. A.* **89,** 4820–4824
14. Ducy, P., and Karsenty, G. (1995) *Mol. Cell. Biol.* **15,** 1858–1869
15. Schinke, T., and Karsenty, G. (1999) *J. Biol. Chem.* **274,** 30182–30189
16. Yang, X., Matsuda, K., Bialek, P., Jacquot, S., Masuoka, H. C., Schinke, T., Li, L., Brancorsini, S., Sassone-Corsi, P., Townes, T. M., Hanauer, A., and Karsenty, G. (2004) *Cell* **117,** 387–398
17. Komori, T. (2006) *J. Cell. Biochem.* **99,** 1233–1239
18. Franceschi, R. T., Ge, C., Xiao, G., Roca, H., and Jiang, D. (2007) *Ann. N. Y. Acad. Sci.* **1116,** 196–207

19. Delépine, M., Nicolino, M., Barrett, T., Golamaully, M., Lathrop, G. M., and Julier, C. (2000) *Nat. Genet.* **25,** 406–409
20. Harding, H. P., Zeng, H., Zhang, Y., Jungries, R., Chung, P., Plesken, H., Sabatini, D. D., and Ron, D. (2001) *Mol. Cell* **7,** 1153–1163
21. Biason-Lauber, A., Lang-Muritano, M., Vaccaro, T., and Schoenle, E. J. (2002) *Diabetes* **51,** 2301–2305
22. Iyer, S., Korada, M., Rainbow, L., Kirk, J., Brown, R. M., Shaw, N., and Barrett, T. G. (2004) *Acta Paediatr.* **93,** 1195–1201
23. Wei, J., Sheng, X., Feng, D., McGrath, B., and Cavener, D. R. (2008) *J. Cell. Physiol.* **217,** 693–707
24. Murakami, T., Saito, A., Hino, S., Kondo, S., Kanemoto, S., Chihara, K., Sekiya, H., Tsumagari, K., Ochiai, K., Yoshinaga, K., Saitoh, M., Nishimura, R., Yoneda, T., Kou, I., Furuichi, T., Ikegawa, S., Ikawa, M., Okabe, M., Wanaka, A., and Imaizumi, K. (2009) *Nat. Cell Biol.* **11,** 1205–1211
25. Zhang, P., McGrath, B., Li, S., Frank, A., Zambito, F., Reinert, J., Gannon, M., Ma, K., McNaughton, K., and Cavener, D. R. (2002) *Mol. Cell. Biol.* **22,** 3864–3874
26. Yamaguchi, A., Komori, T., and Suda, T. (2000) *Endocr. Rev.* **21,** 393–411
27. Harding, H. P., Zhang, Y., Zeng, H., Novoa, I., Lu, P. D., Calfon, M., Sadri, N., Yun, C., Popko, B., Paules, R., Stojdl, D. F., Bell, J. C., Hettmann, T., Leiden, J. M., and Ron, D. (2003) *Mol. Cell* **11,** 619–633
28. Dever, T. E., Feng, L., Wek, R. C., Cigan, A. M., Donahue, T. F., and Hinnebusch, A. G. (1992) *Cell* **68,** 585–596
29. de Haro, C., Méndez, R., and Santoyo, J. (1996) *FASEB J.* **10,** 1378–1387
30. Ducy, P., Zhang, R., Geoffroy, V., Ridall, A. L., and Karsenty, G. (1997) *Cell* **89,** 747–754
31. Xiao, G., Jiang, D., Ge, C., Zhao, Z., Lai, Y., Boules, H., Phimphilai, M., Yang, X., Karsenty, G., and Franceschi, R. T. (2005) *J. Biol. Chem.* **280,** 30689–30696
32. Saito, A., Hino, S., Murakami, T., Kanemoto, S., Kondo, S., Saitoh, M., Nishimura, R., Yoneda, T., Furuichi, T., Ikegawa, S., Ikawa, M., Okabe, M., and Imaizumi, K. (2009) *Nat. Cell Biol.* **11,** 1197–1204
33. Siu, F., Chen, C., Zhong, C., and Kilberg, M. S. (2001) *J. Biol. Chem.* **276,** 48100–48107